Materials Today Communications 26 (2021) 101855

Contents lists available at ScienceDirect

Materials Today Communications

journal homepage: www.elsevier.com/locate/mtcomm

First-principles calculations to investigate the structural, electronic, elastic, vibrational and thermodynamic properties of the full-Heusler alloys X_2ScGa (X = Ir and Rh)

Murat Çanlı [a,*], Esin İlhan [b], Nihat Arıkan [c]

[a] Department of Chemistry and Chemical Processing Technologies, Kırşehir Ahi Evran University, 40500, Kırşehir, Turkey
[b] Department of Architecture, Faculty of Engineering and Architecture, Kırşehir Ahi Evran University, 40200, Kırşehir, Turkey
[c] Department of Medical Services and Techniques, Osmaniye Korkut Ata University, 80010, Osmaniye, Turkey

ARTICLE INFO

Keywords:
Ab-initio
Electronic band structure
Elastic constants
Phonon
Thermodynamic properties

ABSTRACT

This study has investigated ab initio pseudopotential calculations on the structural, electronic, elastic, vibrational and thermodynamic properties of the full-Heusler X_2ScGa (X = Ir and Rh) alloys. The calculations have taken place under consideration of the generalized gradient approximation (GGA) of the density functional theory (DFT) with using the plane-wave *ab initio* pseudopotential method. According to the calculations, the major contribution to electronic states at the Fermi energy has been achieved by d orbitals, revealing a more active role for transition metals Ir (Rh) and Sc atoms. The reckonings point out that the Ir_2ScGa and Rh_2ScGa have metallic behavior at the equilibrium lattice constant with the density of states (DOS) at the Fermi level ($N(EF)$) of 1.412 states/eV and 1.821 states/eV, respectively. The results of the elastic constants showed that these compounds met the criteria for Born mechanical stability. It was also observed that they have a ductile structure and exhibit anisotropic behavior according to Pugh criteria. Besides, the full phonon spectra and their projected partial density of states of the alloys have been analyzed with the first-principle linear-response approach of the density-functional perturbation theory. All the alloys behaved dynamically stable in the $L2_1$ phase. Furthermore, internal free energy, entropy, specific heat capacity at constant volume and vibrational free energy changes of Ir_2ScGa and Rh_2ScGa alloys were analyzed and discussed between the temperature range of 0–800 K using the quasi harmonic approximation. According to the results, these alloys are potential candidate for industrial use.

1. Introduction

Recent research efforts showed that Heusler alloys are still in the attention of many researchers with nearly 15,000 studies because of their great potential in manufacturing ferromagnetic materials for energy applications [1–4]. Fritz Heusler discovered that non ferromagnetic X, Y, and Z elements could be combined to create a ferromagnetic X_2YZ alloy such as Cu_2MnAl. As ternary intermetallic compounds, full-Heusler alloys have a cubic structure. Further, full-Heusler type alloys with the corresponding stoichiometric combinations of X_2YZ, where X and Y are transition metal elements and Z is the main group element [2,3,5].

Among the semi-metallic materials, Heusler alloys have interesting physical properties caused by their capability of 100 % spin polarization and adjustable magnetic behavior [6,7]. While most of the spin bands confirm metallic character, the minority of the spin bands shows semiconductor/insulation behavior with a gap at the Fermi level [8]. Besides, Heusler alloys can turn back to their first shape as magnetic shaped memory after external sources like thermal and mechanical processes. The half-metallic character also gives Heusler alloys the ability to be used for decreasing electric power consumption and increasing integration densities [9].

Ternary Heusler alloys with their half-metallic states at high Curie temperatures (TC) reflect fully spin-polarized currents finding usage in the field of spintronics [10] and spin injection devices such as tunneling magnetic resonance (TMR), giant magnetoresistance (GMR) [1,11], magnetic refrigeration process [12], superconductive materials [13], topological purposes [14,15].

Since most of the Heusler alloys are half-metallic, full-Heusler alloys (X_2YZ) crystallize as in $L2_1$ (#225) structure. Their space group can be in the form of either $Fm\bar{3}m$ [16–18]. Crystallization in full-Heusler alloys

* Corresponding author.
E-mail address: muratbdm@gmail.com (M. Çanlı).

https://doi.org/10.1016/j.mtcomm.2020.101855
Received 26 August 2020; Received in revised form 16 October 2020; Accepted 2 November 2020
Available online 11 November 2020

happen either in the way of 3d electron number in X atom is more than in Y atom in which X, Y, and Z atoms are at Wyckoff positions 8c (1/4, 1/4, 1/4), 4a (0, 0, 0) and 4b (1/2, 1/2, 1/2), respectively, or 3d electron number of Y atom is more than of X atom in which X atoms are located to 4a (0, 0, 0) and 4c (1/4, 1/4, 1/4), Y and Z atoms are placed at 4b (1/2, 1/2, 1/2) and 4d (3/4, 3/4, 3/4) positions, respectively [19].

Any atomic disorder in the lattice site distributions of Heusler alloys can strongly influence their electronic structures, their magnetic and transport properties with a tremendous difference [20–22]. Even though formation enthalpies, magnetic properties, and structural stability of some full-Heusler alloys have already been in the focus of experimental studies so far, computational methods (quantum mechanics) have more appropriate tools to find out the best compositions and properties of many alloys with different configuration which is not possible to synthesize in real.

The formation enthalpy and lattice parameters of a serial Heusler alloy were also determined using the first-principle calculations by Gilleßen and Dronskowski [23]. Their results showed that only 12 % of 810 Heusler alloys were able to be synthesized experimentally. While significant advances in theoretical explanations of some physical properties of X_2ScGa (X = Ir and Rh) alloys are likely, most of their dynamic properties are still not fully determined. Full phonon distribution curves are required to understand lattice dynamics microscopically. In addition, the phonon spectrum information plays an important role in determining various material properties such as phase transition, thermodynamic stability, transport, and thermal properties.

Elastic properties are important for the determination of the strength and hardness of the materials because the elastic constants show how the material responds to interatomic forces, electron-phonon interactions, phase transition, and transport coefficients as a function of the bulk and shear modulus [24], just like specific heat, thermal expansion, Debye temperature, Gruneisen parameter, and melting point [25]. Thermodynamic properties also help to figure out the heat absorption capacity of the alloy which gives insight about phase transitions, phase diagram, and endurance against temperature [26]. In addition, elastic and phonon properties of the alloys give insight about their potential for whether being used as shape memory materials [27].

Iridium (Ir) based alloys already have a usage in spintronic devices, memory storage devices, TMR, and GMR. Recent studies about Ir_2CrAl, Ir_2MnSi, Ir_2VGa, Ir_2VGe, Ir_2MnAl, Ir_2ScSi, Ir_2ScGe, and Ir_2ScSn pointed out the existence of their high spin polarization capacity at the Fermi level [28–32]. In addition to Ir, Rhodium (Rh) based alloys such as Rh_2MnBi, Rh_2MnAl, Rh_2FeAl, Rh_2CrSb, Rh_2CrAl, Rh_2CrIn, Rh_2FeGa and Rh_2FeIn were studied by several researchers [33,34]. Just like in Ir-based alloys, these studies refer to that those Rh-based alloys have similar electronic and structural properties for spintronic applications.

The accuracy and efficiency of the density functional theory (DFT) are achieved computationally with a consecutive improvement of correlation in which the first step is the local-density approximation (LDA), and the second one is the generalized gradient approximation (GGA) [35]. In this study, because of its advantages as being accepted an accurate approach the generalized gradient approximation (GGA) of the density functional theory (DFT) was used for calculation of elastic and phonon properties of Ir_2ScGa and Rh_2ScGa full-Heusler alloys with using the plane-wave ab initio pseudo-potential method for the first time. The GGA has been estimated by a widely used parametrization of Perdew, Burke, and Ernzerhof (PBE) [36]. The mesh constants and formation enthalpies of the $ScGaIr_2$ and $ScGaRh_2$ alloys were calculated with the VASP code [37].

In this paper, while Section 2 is dedicated to the description of calculation methods, the results for the structural, electronic, elastic, vibrational and thermodynamic properties of $ScGaX_2$ (X = Ir and Rh) alloys is presented in Section 3. A final brief is given in Section 4.

2. Method

The calculations were performed via the ab initio plane wave pseudopotential method operated in the Quantum-Espresso package [38,39]. The exchange correlation function was calculated using the generalized gradient approach (GGA) parameterized by Perdew-Burke-Ernzerhof (PBE) [36]. The wave functions were extended in plane waves with a 40 Ry kinetic energy cut (a kinetic energy cut-off of 40 Ry) for Ir_2ScGa and Rh_2ScGa. Electronic charge intensity was taken into consideration up to 400 Ry of kinetic energy cut-off. To get precise results, convergence threshold was taken as 10–9 Ry with mixing beta of 0.7. Energy convergence of 1 mRy per atom has been satisfied by using $10 \times 10 \times 10$ Monkhorst – Pack [40] grid of k-points for sampling of the Brillouin zone (IBZ).

The Ab initio pseudopotential method serves to make total energy calculations for arbitrary crystal structures. Thus, the small strain of the equilibrium lattice was applied to observe the change in the total energy for finding the elastic constants. Elastic constants are characterized in proportion to the second order coefficient of total energy in a polynomial fit as a function of the distortion parameter δ.

Three independent elastic constants, such as C_{11}, C_{12} and C_{44}, for cubic crystals, are used and need three equations to get them. The bulk module (B), which depends on the values of C_{11} and C_{12}, was calculated as in the following equation.

$$B = (C_{11} + 2C_{12})/3 \tag{1}$$

Here, the bulk module is determined as a measure of how resistant a material can be under an external pressure.

The tetragonal shear modulus contains a volume-conserving deformation for determining C_{11} - C_{12} as the next step.

$$\overline{\varepsilon} = \begin{pmatrix} \delta & 0 & 0 \\ 0 & \delta & 0 \\ 0 & 0 & (1+\delta)^{-2} - 1 \end{pmatrix} \tag{2}$$

This strain leads to an energy change as $\Delta E = 3V_o\ (C_{11}\text{-}C_{12})\delta^2 + O[\delta^3]$.

The last step defines a volume-conserving base-centered orthorhombic strain tensor.

$$\overline{\varepsilon} = \begin{pmatrix} 0 & \delta/2 & 0 \\ \delta/2 & 0 & 0 \\ 0 & 0 & \dfrac{\delta^2}{(4-\delta)^2} \end{pmatrix} \tag{3}$$

This strain runs the change in energy as $\Delta E = 1/2C_{44}Vo\delta^2 + O[\delta^4]$.

With determination of the second order elastic constants for Ir_2ScGa and Rh_2ScGa alloys, there is an opportunity to use the Voigt-Reuss-Hill (VRH) averaging approach [41–43] for calculation of the polycrystalline elastic module.

The shear modulus presented with G is defined as the shear stress to shear strain ratio:

$$G_v = \frac{C_{11-}C_{12} + 3C_{44}}{5}, G_R = \frac{5C_{44}(C_{11} - C_{12})}{3(C_{11} - C_{12}) + C_{44}}, G_H = \frac{G_V + G_R}{2} \tag{4}$$

Young's module (E), which is known as an indicator of hardness for materials, is determined from bulk module (B) and shear module (G) and given as follows:

$$\mathrm{E} = \frac{9BG}{(3B + G)} \tag{5}$$

The anisotropy factor (A) for cubic symmetry crystals defines the degree of anisotropy compared to the isotropic material significant for engineering and is given in the following case:

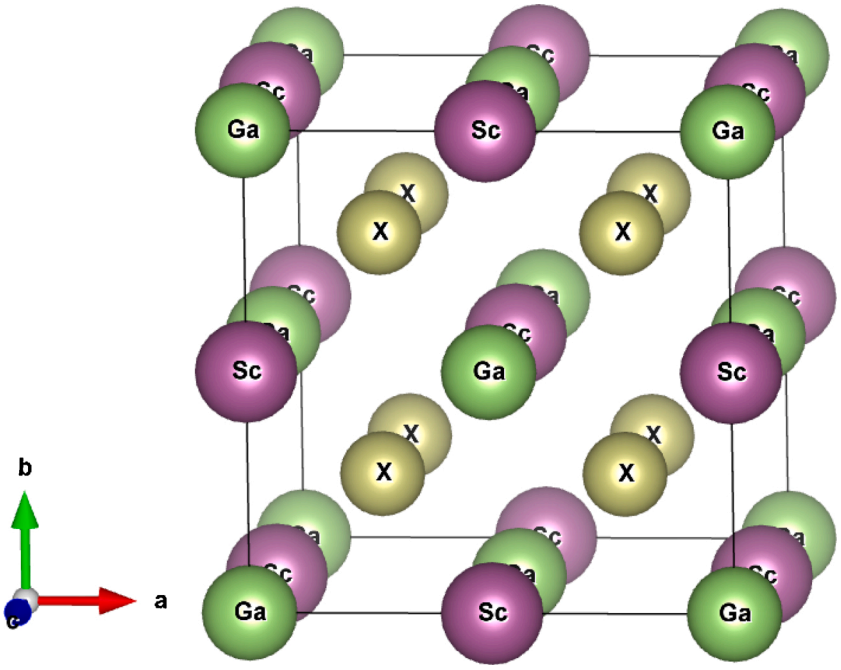

Fig. 1. Crystal structure of X_2ScGa (X = Ir and Rh) alloys in the L21 phase.

$$A = \frac{2C_{44}}{(C_{11} - C_{12})} \tag{6}$$

The ratio (σ) of Poisson as the elongation ratio of lateral contraction gives detailed information about the bonding quality of a material as follows:

$$\sigma = \frac{1}{2}\left(1 - \frac{E}{3B}\right) \tag{7}$$

Finally, the Debye temperature (θ_D) is estimated from the equation below:

$$\theta_D = \frac{h}{k}\left(\frac{3n}{4\pi}\,\frac{N_A\rho}{M}\right)^{1/3} V_m \tag{8}$$

where h, k, n, N_A, ρ and M, are Planck's constant, Boltzmann's constant, the atomic number of the molecule, Avogadro's number, the mass density, and the molecular weight, respectively.

Baroni et al. [DFPT] [44] utilized the density functional perturbation theory provided by [45] for calculation of lattice dynamics. Eight dynamic matrices were determined on a 4 × 4 × 4 q network to find the full phonon spectra and intensity of states. Fourier deconvolution was used to evaluate dynamic matrices in random wave vectors. From the calculated phonon frequencies and DOS, constant volume specific temperature (C_v) against temperature was found by quasi harmonic approach (QHA) [46].

In addition to all this, the corresponding calculations with a GGA + U (Hubbard coefficient) scheme for the electronic correlation function [47,48] were performed to show the electronic correlations in electrons for Ir, Rh and Sc atoms in the Ir_2ScGa and Rh_2ScGa alloys. In the GGA + U calculations, effective U values of 3 eV were adopted for Ir, Rh and Sc.

3. Results

3.1. Structural properties

X_2ScGa (X = Ir and Rh) alloys are in Cu_2MnAl ($L2_1$ phase) type structure and crystallize in a cubic phase with Fm $\overline{3}$ m symmetry group as shown in Fig. 1. The minimum ground state energy was obtained by optimizing the unit cell structure within the GGA functional scheme. As a first step, equilibrium lattice constants are determined by minimizing the total energy corresponding to the different values of lattice constants as presented in Table 1. Thus, the lattice constant values in this study for both alloys are found in good agreement with the current theoretical results [36,49].

In addition to the calculations carried out with the GGA meteo, the lattice constant value with the GGA + U approach was also calculated. The GGA + U results for both alloys were 0.28 % and 0.24 % higher for Ir_2ScGa and Rh_2ScGa, respectively, than the GGA results. However, there was no experimental data found to compare with the calculated

Table 1
The calculated lattice constants (a_0), bulk modulus (B), elastic constants (C_{ij}) and formation energy (ΔH_f) of Ir_2ScGa and Rh_2ScGa alloys.

Materials	References	a_0 (Å)	B (GPa)	C_{11} (GPa)	C_{12} (GPa)	C_{44} (GPa)	ΔH_f (eV/atom)
	This work (GGA)	6.256	224.190	293.407	189.582	120.198	−0.781
	This work (GGA + U)	6.274	185.733	244.308	156.445	99.303	
Ir_2ScGa	Vasp-GGA [26]	6.263					−0.795
	Theory [27]	6.257					
	Vasp-GGA [50]	6.269	191	281	146	103	−0.804
	This work (GGA)	6.234	165.402	248.261	123.972	84.092	−0.953
	This work (GGA + U)	6.249	158.972	242.786	117.065	77.454	
Rh_2ScGa	Vasp-GGA [26]	6.236					−0.982
	Theory [27]	6.225					
	Vasp-GGA [50]	6.255	161	261	111	80	−0.986

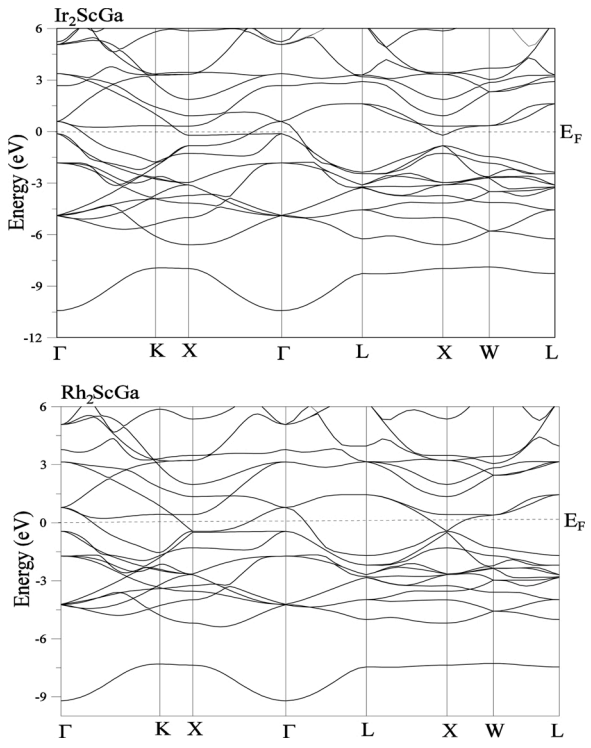

Fig. 2. Electronic band structures of X_2ScGa (X = Ir and Rh) alloys along the selected lines of high symmetry.

mesh constants. The other structural parameter calculated and presented in Table 1 was the bulk modulus. Bulk modulus is a structural constant to explain how resistant a material is against compression. In this case, the bulk modulus value of Ir_2ScGa is greater than the value of Rh_2ScGa. This means that the compressive strength of Ir_2ScGa was determined higher than that of Rh_2ScGa. On the other hand, there is no comparable yield in the available data for the bulk modulus values calculated for both alloys. Both GGA and GGA + U calculations have shown that both alloys are non-magnetic. Also, the previous calculations confirm the magnetic nature of these alloys [34,36].

There are also formation energy calculations which are used as an important parameter to verify the chemical stability and possible experimental synthesizability of the proposed full Heusler alloys Ir_2ScGa and Rh_2ScGa. The formula used for such calculations is:

$$E_{For} = (2E_{Ir\,(Rh)} + E_{Sc} + E_{Ga}) - E_{Ir\,(Rh)_2ScGa} \quad (9)$$

Here, $E_{Ir\,(Rh)_2ScGa}$ is the total energies of the Ir_2ScGa and Rh_2ScGa alloys, and $E_{Ir\,(Rh)}$, E_{Sc} and E_{Ga} are the energy of each atom in the bulk form, respectively. As can be seen in the computed negative formation energy value, these alloys are thermodynamically stable and may be synthesized experimentally. The calculated negative values of formation enthalpy (-0.781 eV / atom for Ir_2ScGa and -0.953 eV / atom for Rh_2ScGa) indicate that the alloys are structurally stable and experimentally synthesizable. The calculated formation energy values are quite compatible with VASP [50] calculations.

3.2. Electronic properties

Valence electrons of a material are an important quantity for understanding the electronic band properties of the related material in detail. According to the high symmetry aspects of Ir_2ScGa and Rh_2ScGa electronic band structures in Brillouin region presented in Fig. 2, the band profiles of both alloys are similar. The electronic band profiles of both alloys do not contain any band gap at the Fermi energy level. This means the existence of metallic behavior for both alloys. In addition to the electronic band structure, the density of states (DOS) graphics is presented in Fig. 3 to understand the electronic contributions of these alloys more clearly. As shown in Fig. 3 and supports the electronic band profile (Fig. 2), both alloys have finite state densities at Fermi Level. Therefore, no gaps were found in the Fermi energy level, and the finite total densities of the states were found to be 1.412 sates / eV per unit cell for Ir_2ScGa and 1.821 states / eV for Rh_2ScGa. The major contribution to the Fermi energy level for both materials comes from the Ir-5d (Rh-4d) electrons and Sc-3d electrons, while there is an effect of Ga-d electrons on the Fermi level. In other words, the metallic character of these materials is tracked from the d states of Ir and Sc atoms for Ir_2ScGa and the d states of Rh and Sc atoms for Rh_2ScGa. There is a sharp peak of Sc-3d orbitals around 3 eV for both materials. On the other hand, there is another sharp peak located around −3 eV, just below the Fermi energy level because of Ir-5d states for Ir_2ScGa and Rh-4d states for Rh_2ScGa. Thus, with previous studies with the same phase and the same space group [51–53] it can be said that the data is in harmony.

3.3. Elastic properties

Elastic constants of a crystal can provide important and detailed information to analyze the response of solids to external stresses for their mechanical and structural stability [54,55]. In this part, the elastic constants (C_{ij}), bulk module (B), shear modulus (G), B/G ratio, Young's module (E), Poisson's ratio (σ) and anisotropic factor (A) of the Ir_2ScGa and Rh_2ScGa alloys were calculated. Standard mechanical stability [56] requirements for a cubic crystal are as follows:

$$C_{11}>0,\ C_{11}\text{-}C_{12}>0,\ C_{11}+2C_{12}>0 \text{ and } C_{44}>0 \quad (10)$$

In the calculations, the major focus was on the mechanical and structural stability of Ir_2ScGa and Rh_2ScGa alloys in the $L2_1$ phase. There was no comparison made with the calculated elastic constants of the alloys studied here because of lacking background theoretical or experimental data in literature. The results obtained within the scope of the GGA method and GGA + U approach are presented in Table 1. According to the stability criteria, the alloys examined with both GGA method and GGA + U approach were found mechanically stable because the Cauchy pressure (C_{11} - C_{12}) value was positive for the two alloys. In addition, mechanical properties such as bulk modulus, shear modulus, Young modulus, Pugh ratio B/G, Anisotropic factor, Poisson ratio and Cauchy pressure (CP), related to elastic constants were found with Voigt-Reuss-Hill approach from Eqs. (1), (4)–(7) in Table 2.

Here, Ir_2ScGa is more resistant to pressure deformation than Rh_2ScGa. Pugh ratio (B/G) is an important parameter used to reveal the brittle or ductile nature of the material. Fort his study, the ratio of Pugh (B/G) indicates that both materials have a ductile nature, because if B/G < 1.75, the material is claimed to be brittle, and if B/G > 1.75, the material is said to be ductile. The ductile structure is further verified by the value of the Poisson's ratio, which also measures the ductility and brittleness of materials. The values of 0.32 and 0.30 for Ir_2ScGa and Rh_2ScGa, respectively, are greater than the critical value of 0.26, which distinguishes ductility from brittleness. Moreover, positive values of Cauchy pressure ($C_{12} - C_{44}$) in both alloys support the ductile character of these alloys. On the other hand, Cauchy pressure (C_{12}-C_{44}) can also be used to define the character of atomic bonding of materials. While a negative value of the Cauchy pressure (C_{12}–C_{44}) shows the covalent nature of a material, positive values of the Cauchy pressure point out directional metallic bonding in the material.

Here, the positive Cauchy pressure values calculated for both GGA and GGA + U revealed the metallic nature of both alloys. Type of atomic bonding is also determined by Poisson's ratio. The Poisson ratio (σ) helps to present the type and compressibility of the bonding forces in the material. If the Poisson ratio is either 0.1, 0.25 or 0.33, the bonding nature of the materials between atoms are called covalent, ionic, and metallic bond, respectively. In this study, because of the calculated

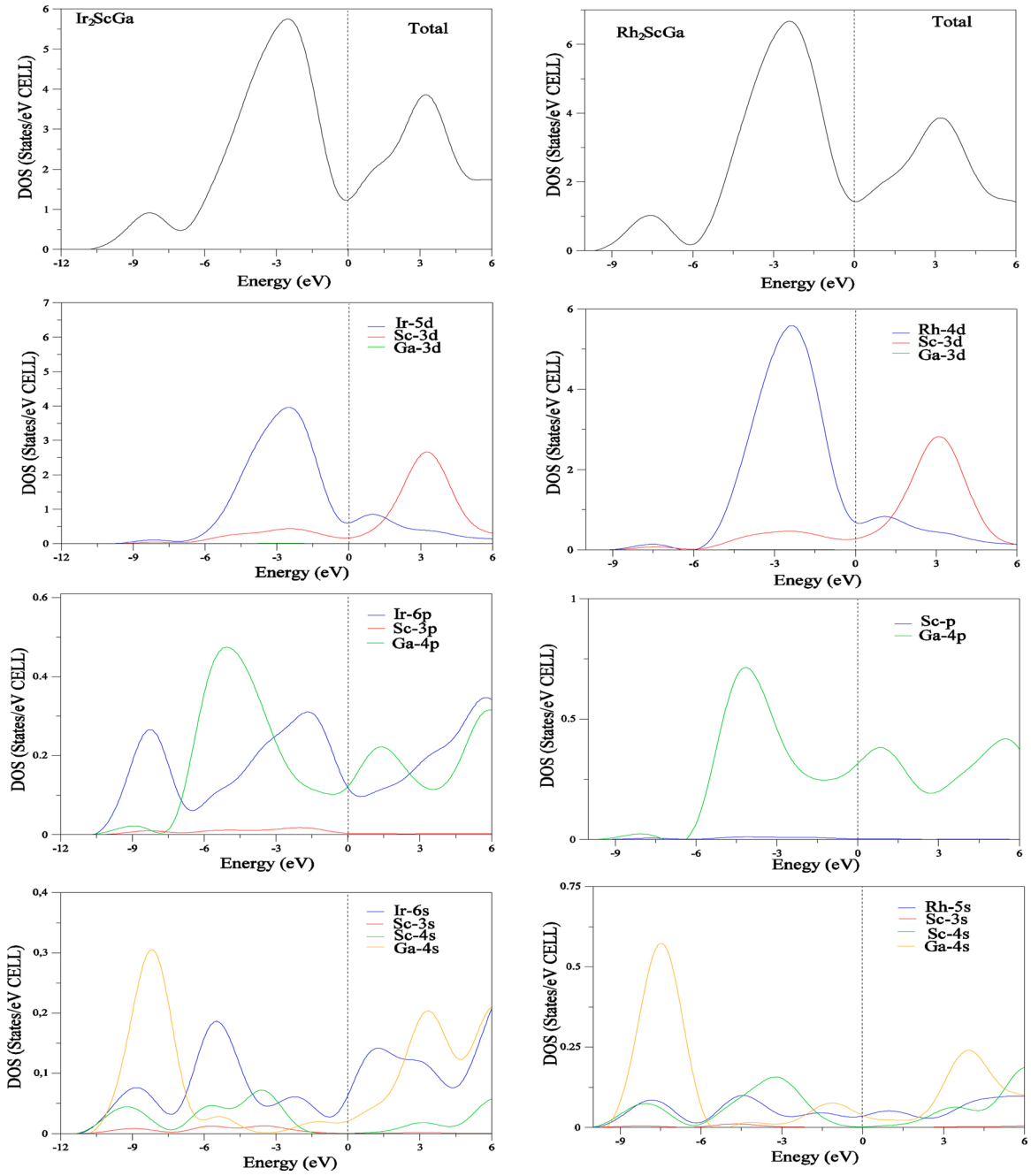

Fig. 3. The electronic total and partial density of states of X_2ScGa (X = Ir and Rh) alloys.

Table 2
Bulk moduli (B) and Shear modulus (G) with subscripts R and V based on the Reuss and the Voigt averages, B/G ratios, anisotropy factors (A), Young's moduli (E), and Poisson's ratios (σ) Debye temperature and Cauchy Pressure (CP) of Ir_2ScGa and Rh_2ScGa alloys.

Materials	References	B (GPa)	G (GPa)	B/G	A	E (GPa)	σ	θ_D (K)	$C_P=C_{12}-C_{44}$
Ir_2ScGa	This work(GGA)	224.190	85.821	2.612	2.315	228.173	0.32	324.14	69.384
	This work (GGA + U)	185.733	71.586	2.594	2.260	190.194	0.32	306.405	57.142
	Vasp-GGA [50]	191	87	2.195	–	226.48	30	–	43
Rh_2ScGa	This work	165.402	74.498	2.220	1.353	194.317	0.30	326.02	39.880
	This work (GGA + U)	158.972	71.244	2.231	1232	185.954	0.30	307.024	39.611
	Vasp-GGA [50]	161	78	2.064	–	201.38	29	–	30

Poisson ratio values are close to 0.33, both materials have a metallic band character. In another factor, isotropy degree of the crystal depends on how anisotropy factor (A) is close to 1, but any lower or higher values of anisotropy from 1 shows the deviation level of crystallinity. The calculated anisotropy values of the Ir_2ScGa and Rh_2ScGa alloys are 2.315 (2.260 for GGA + U) and 1.353 (1.232 for GGA + U) respectively, and they point out the elastically anisotropic nature. The reason for that is the high dependence of the alloys on C_{44}.

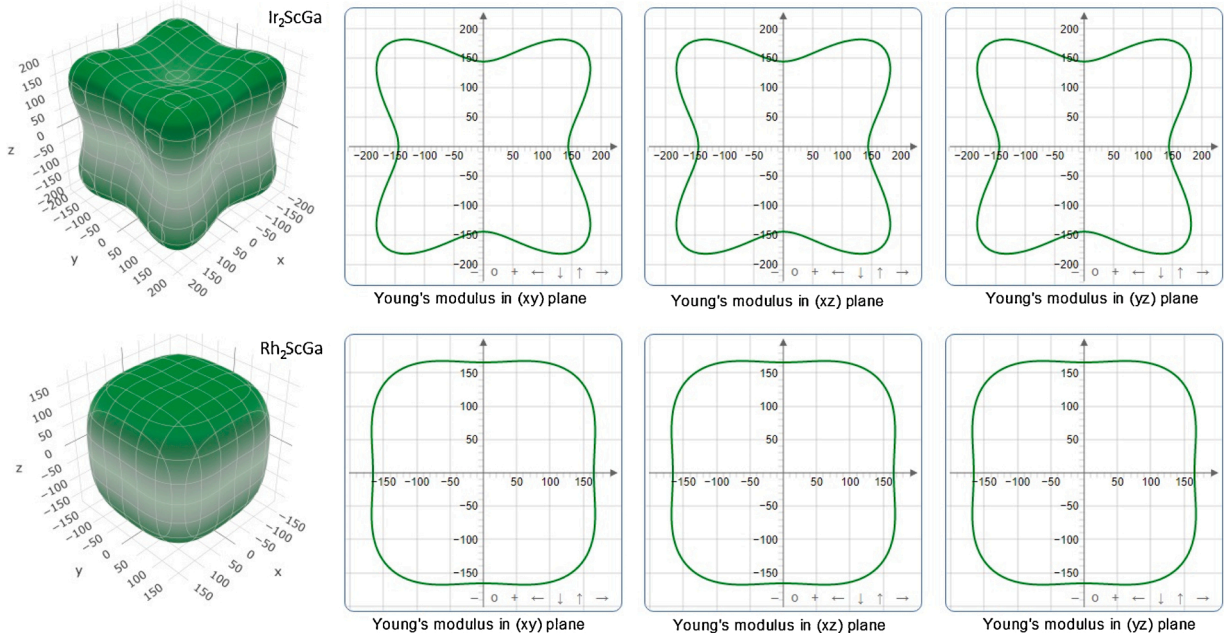

Fig. 4. Three-dimensional (3D) and two-dimensional (2D) directional dependence of the Young's moduli of X2ScGa (X = Ir and Rh) alloys in the L21 phase.

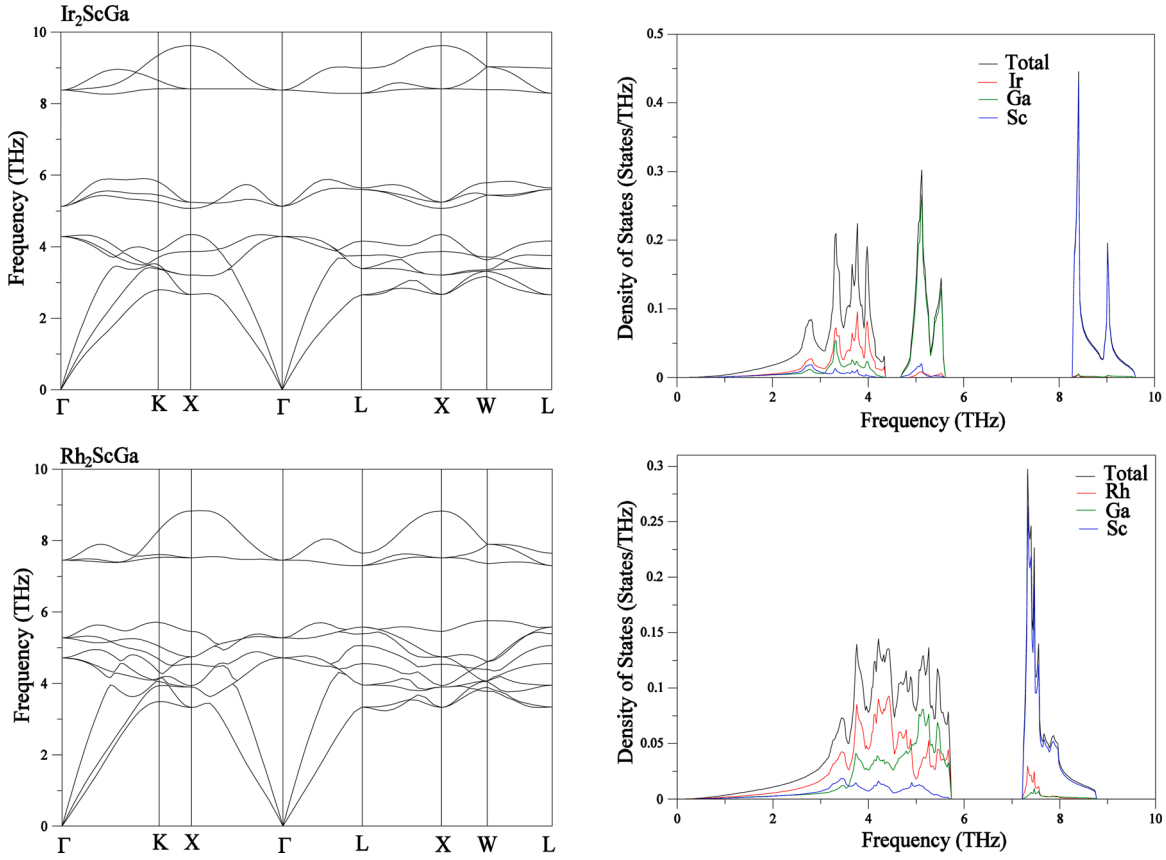

Fig. 5. (a) Calculated full phonon spectra for X_2ScGa (X = Ir and Rh) alloys, (b) Calculated total and partial phonon densities of states for X_2ScGa (X = Ir and Rh) alloys.

The measure of the stiffness of the alloys can be evaluated using the Young module (E). The higher the Young module of a material, the higher the deformation resistance. In lights of the Young module values, Ir_2ScGa alloy is stiffer than the Rh_2ScGa alloy. The dependence of Young's modulus in both 2D and 3D directions was calculated using the ELATE [56] package program for both materials, and the results are shown in Fig. 4. If the shape is spherical, the material is known as an isotropic material. Anisotropy shows the amount of deviation on the surfaces. Both alloys are anisotropic in all planes, and Ir_2ScGa has a higher anisotropy. On the other hand, there is no clue of the

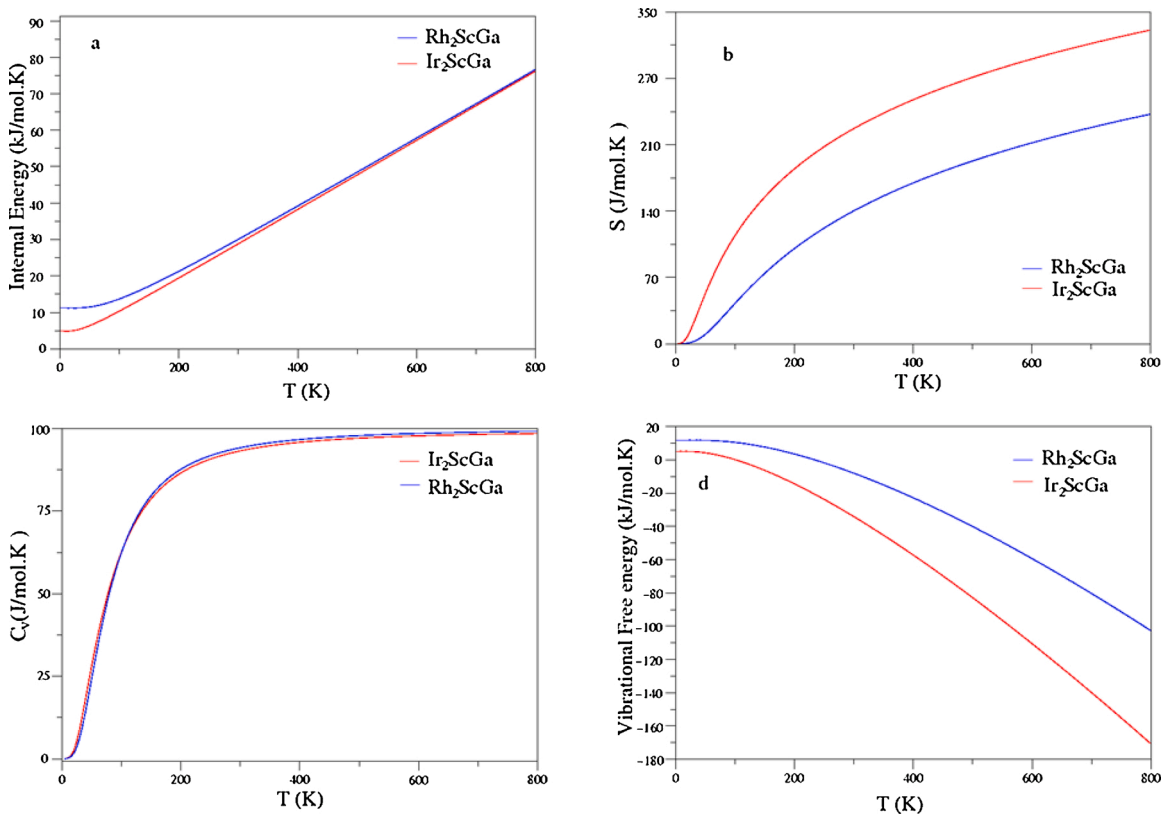

Fig. 6. The temperature dependence of (a) Internal energies (b) Entropies (c) Constant volume heat capacities and (d) Vibrational free energies of X_2ScGa (X = Ir and Rh) alloys.

experimental values for comparing the elastic constants of Ir_2ScGa and Rh_2ScGa. Consequently, the present study is in good agreement with the theoretical values calculated by VASP-GGA [57] for the elastic constants and related parameters of both alloys. Finally, there is another quantity calculated, called micro-hardness parameter (H). The microhardness value is presented as follows $H = [(1-2\sigma)\ E] / 6\ (1 + \sigma)$. The H values calculated for the Ir_2ScGa and Rh_2ScGa alloys were 10.371 GPa and 9.964 GPa, respectively.

3.4. Phonon properties

The phonon can be defined as a unit of vibrational energy in the periodic, elastic arrangement of atoms or molecules within a crystal in condensed matter physics. One of the important parameters representing the stable phase of a material can be determined from the lattice dynamic properties of that material. To calculate the phonon dispersion curves for Ir_2ScGa and Rh_2ScGa alloys in the $L2_1$ cubic phase, the linear response method in the density functional perturbation theory was used and the resulting phonon dispersion curves are shown in Fig. 5a. There is no imaginary part in the full-phonon curves of Ir_2ScGa and Rh_2ScGa alloys in $L2_1$ type cubic structure. This evidence shows the dynamic stability in both alloys. For each alloy, the phonon spectra in the entire frequency range can be divided into upper high frequency modes called an optical branch and low frequency branch modes called an acoustic branch. In the $L2_1$ cubic phase, the primitive unit cell of Ir_2ScGa and Rh_2ScGa alloys consists of four atoms having 12 phonon branches. Among these 12 phonon branches, there are three acoustic branches having two transverse (TA) and one longitudinal (LA) branch and nine optical branches with three longitudinal optics (LO) and six transverse optical (TO) branches. In the two alloys, there has been the phonon band gap detected because of separation of the upper optical branches from the other phonon branches, as presented in Fig. 5-a and b.

The bandwidth values were calculated as 0.299 and 2.631 THz for Ir_2ScGa and 1.472 THz for Rh_2ScGa, respectively. This side of the alloys can lead them to be used in various applications such as phonon tape gaps, sound filters and mirrors. Due to the void, the sound does not spread and only reflects from the surface [50,58]. Such features can be ideal for use in both insulators and mirrors. On the other hand, the optical phonon frequencies at the zone center (Γ-point) were measured as 4.280, 5.159 and 8.384 THz for Ir_2ScGa, and 4.596, 5.266 and 7.425 THz for Rh_2ScGa. To examine better the full phonon spectra in more detail, the total and fragmented phonon state density were drawn and given in Fig. 5-b. The light Sc atoms caused the highest phonon frequencies in the two alloys. Near approximately 5–6 THz, vibration frequencies can be seen originating from Ga atoms. As clearly seen in Fig. 5-b, heavier Ir and Rh atoms headed to overlapping acoustic and lower optical modes. The calculated phonon frequencies of the materials among the dynamic properties of these alloys were considered as unique because of lacking available literature data.

3.5. Thermodynamic properties

Several thermodynamic properties such as internal energy, vibration energy, entropy and specific heat capacity were examined at a temperature between 0 and 800 K using the phonon DOS within the framework of the Quasi-harmonic approach (Fig. 6a–d). In Fig. 6a–c, the internal energy, entropy, and specific heat capacity increased with raising temperature as a temperature function for X_2ScGa (X = Ir and Rh). On the other hand, vibration free energy changed with temperature as a reverse function of temperature (Fig. 6.d). The relationship between specific heat and temperature had a linear alteration rapidly up to 200 K, and then, for higher temperatures, it remained constant at a limit value known as the Dulong-Petit limit. Here, N is the number of atoms in the unit cell, and R is the ideal gas constant. The increase in entropy is directly related to the radius of the X (X = Ir and Rh) atom of the alloys. Since the atomic radius of the Ir atom is larger than the atomic radius of

the Rh atom, the entropy value increases faster for the Ir alloy. One of the important thermodynamic properties for a solid is Debye temperature, which provides information about many quantities such as phonons, thermal expansion, thermal conductivity, heat capacity, melting temperature, lattice enthalpy and elastic hardness. Debye temperature θ_D is considered the highest temperature of a solid's normal vibration mode (maximum thermal vibration frequency). The Debye temperatures calculated for both alloys are close to each other (Table 2).

4. Conclusions

This study has investigated ab initio pseudopotential calculations under consideration of the generalized gradient approximation (GGA) of the density functional theory (DFT)on the structural, electronic, elastic, vibrational and thermodynamic properties of the full-Heusler X_2ScGa (X = Ir and Rh) alloys. Systematic theoretical studies on the electronic, elastic, vibrational and thermodynamic properties of the X_2ScGa (X = Ir and Rh) Heusler alloys were carried out for the first time, using the first principle calculations based on the density functional theory with using the plane-wave *ab initio* pseudopotential method. The calculations show that both alloys are mechanically, dynamically, and thermodynamically stable. The calculated electronic band structure and the associated DOS point out a metallic nature in their two alloys. The contribution of conductivity to the fermi energy level comes from Ir-d and Sc-d electrons for Ir_2ScGa and Rh-d and Sc-d electrons for Rh_2ScGa. Elastic constants and related quantities such as Cauchy pressure, anisotropy, Pugh ratio, and Poisson ratio have implicated both alloys as ductile and having metallic band character with anisotropic behavior. Since these alloys meet the Born stability criteria, they have shown mechanical stability. The phonon dispersion curves, and the matching total and partial DOS were first investigated using the linear response approach in the context of the functional perturbation theory. Due to the lack of an imaginary frequency in the full phonon spectrum calculated for both alloys, it was determined that these alloys were dynamically stable in the Heusler phase ($L2_1$). Within the scope of thermodynamic research, the quasi-harmonic approach was used to determine internal free energy, entropy, specific heat capacity at constant volume, and vibrational free energy for different temperatures within the calculated phonon DOS. From the study of the electronic properties, it was predicted that the compounds have metallic and magnetic characters. They are non-half-metallic compounds because of the inexistence of a gap in one of the two spin channels (up or down). Thus, this result is in good agreement with the calculated total spin magnetic of the compounds. Consequently, the variation of thermodynamic properties of these alloys with temperature from 0 to 800 K was applied, and the results showed that these alloys can be used for industrial purposes.

References

[1] F. Kuroda, T. Fukushima, T. Oguchi, First-principles study of magnetism and phase stabilities of V2 based antiferromagnetic Heusler alloys, J. Appl. Phys. 127 (2020) 193904.

[2] Y. Han, Z. Chen, M. Kuang, Z. Liu, X. Wang, X. Wang, 171 Scandium-based full Heusler compounds: a comprehensive study of competition between XA and $L2_1$ atomic ordering, Results Phys. 12 (2019) 435–446.

[3] Y. Han, A. Bouhemadou, R. Khenata, Z. Cheng, T. Yang, X. Wang, Prediction of possible martensitic transformations in all-d-metal Zinc-based Heusler alloys from first-principles, J. Magn. Magn. Mater. 471 (2019) 49–55.

[4] S.A. Sofi, D.C. Gupta, Exploration of electronic structure, mechanical stability, magnetism, and thermophysical properties of $L2_1$ structured Co_2XSb (X = Sc and Ti) ferromagnets, Int. J. Energy Res. 44 (2020) 2137–2149, https://doi.org/10.1002/er.5071.

[5] S.A. Sofi, D.C. Gupta, Investigation of structural, elastic, thermophysical, magneto-electronic, and transport properties of newly tailored Mn-based Heuslers: a density functional theory study, Int. J. Quantum Chem. 120 (2020) e26216, https://doi.org/10.1002/qua.26216.

[6] A. Amudhavalli, M. Manikandan, R. Rajeswarapalanichamy, K. Iyakutti, Electronic and magnetic properties of Fe2− xCoxTiGe (x= 0, 0.5, 1, 1.5, 2) full Heusler alloys, Chinese J. Phys. 59 (2019) 166–174.

[7] F. Semari, F. Dahmane, N. Baki, Y. Al-Douri, S. Akbudak, G. Uğur, C.H. Voon, First-principle calculations of structural, electronic and magnetic investigations of Mn2RuGe1-xSnx quaternary Heusler alloys, Chinese J. Phys. 56 (2) (2018) 567–573.

[8] S.A. Khandy, I. Islam, D.C. Gupta, A. Laref, Full Heusler alloys (Co_2TaSi and Co_2TaGe) as potential spintronic materials with tunable band profiles, J. Solid State Chem. 270 (2019) 173–179.

[9] I. Galanakis, Surface properties of the half-and full-Heusler alloys, J. Phys. Condens. Matter 14 (25) (2002) 6329.

[10] L. Beldi, Y. Zaoui, K.O. Obodo, H. Bendaoud, B. Bouhafs, D° half-metallic ferromagnetism in GeNaZ (Z= Ca, Sr, and Ba) ternary half-heusler alloys: an ab initio investigation, J. Supercond. Nov. Magn. (2020) 1–12.

[11] B. Fadila, M. Ameri, D. Bensaid, M. Noureddine, I. Ameri, S. Mesbah, Y. Al-Douri, Structural, magnetic, electronic, and mechanical properties of full-Heusler alloys Co_2YAl (Y= Fe, Ti): first principles calculations with different exchange-correlation potentials, J. Magn. Magn. Mater. 448 (2018) 208–220.

[12] I. Dubenko, A. Quetz, S. Pandey, A. Aryal, M. Eubank, I. Rodionov, et al., Multifunctional properties related to magnetostructural transitions in ternary and quaternary Heusler alloys, J. Magn. Magn. Mater. 383 (2015) 186–189.

[13] J.H. Wernick, G.W. Hull, T.H. Geballe, J.E. Bernardini, J.V. Waszczak, Superconductivity in ternary Heusler intermetallic compounds, Mater. Lett. 2 (2) (1983) 90–92.

[14] S. Chadov, X. Qi, J. Kübler, G.H. Fecher, C. Felser, S.C. Zhang, Tunable multifunctional topological insulators in ternary Heusler compounds, Nat. Mater. 9 (7) (2010) 541–545.

[15] H. Lin, L.A. Wray, Y. Xia, S. Xu, S. Jia, R.J. Cava, et al., Half-Heusler ternary compounds as new multifunctional experimental platforms for topological quantum phenomena, Nat. Mater. 9 (7) (2010) 546–549.

[16] F. Ahmadian, A. Salary, Half-metallicity in the inverse heusler compounds Sc_2MnZ (Z= C, Si, Ge, and Sn), Intermetallics 46 (2014) 243–249.

[17] K.H.J. Buschow, P.G. Van Engen, Magnetic and magneto-optical properties of Heusler alloys based on aluminum and gallium, J. Magn. Magn. Mater. 25 (1) (1981) 90–96.

[18] S. Ghosh, D.C. Gupta, Electronic, magnetic, elastic and thermodynamic properties of Cu_2MnGa, J. Magn. Magn. Mater. 411 (2016) 120–127.

[19] E.G. Özdemir, E. Eser, Z. Merdan, Investigation of structural, half metallic and elastic properties of a new full-heusler compound - Ir_2MnSi, Chinese J. Phys. 56 (4) (2018) 1551–1558.

[20] S. Picozzi, A. Continenza, A.J. Freeman, Role of structural defects on the half-metallic character of Co_2MnGe and Co_2MnSi Heusler alloys, Phys. Rev. B 69 (9) (2004) 094423.

[21] Y. Miura, K. Nagao, M. Shirai, Atomic disorder effects on half-metallicity of the full-Heusler alloys Co2Cr1-xFex: a first-principles study, Phys. Rev. B 69 (14) (2004) 144413.

[22] K. Hem Chandra, et al., Electronic structure, magnetism and disorder in the Heusler compound Co2TiSn, J. Phys. D Appl. Phys. 40 (6) (2007) 1587.

[23] M. Gilleßen, R. Dronskowski, A combinatorial study of full Heusler alloys by first-principles computational methods, J. Comput. Chem. 30 (8) (2009) 1290–1299.

[24] S. Aouimer, M. Ameri, D. Bensaid, N.E. Moulay, A.Z. Bouyakoub, F.Z. Boufadi, et al., The elastic, electronic and thermodynamic properties of a new Cd based full Heusler compounds–a theoretical investigation using DFT based FP-LMTO approach, Acta Phys. Pol. A 136 (1) (2019) 127–134.

[25] L.Liu C. Chen, Y. Wen, A. Jiang, The structural and elastic properties of a full-Heusler compound Cu2MnAl under pressure, High Temp.-High Press. 49 (4) (2020) 357–366.

[26] Z. Wen, Y. Zhao, H. Hou, B. Wang, P. Han, The mechanical and thermodynamic properties of Heusler compounds Ni2XAl (X= Sc, Ti, V) under pressure and temperature: a first-principles study, Mater. Des. 114 (2017) 398–403.

[27] Y. Sokolovskaya, O. Miroshkina, V. Sokolovskiy, M. Zagrebin, V. Buchelnikov, A. Zayak, A ternary map of Ni-Mn-Ga Heusler alloys from ab initio calculations, arXiv preprint arXiv 09128 (2003) 2020.

[28] G. Forozani, F. Karami, M. Moradi, Structural, electronic, magnetic, and optical properties of Ir2ScZ (Z= Si, Ge, Sn) full-heusler compounds: a first-principles study, J. Electron. Mater. (2020) 1–10.

[29] S. Krishnaveni, M. Sundareswari, M. Rajagopalan, Prediction of electronic and magnetic properties of full Heusler Alloy–Ir2CrAl. IOSR, J. Appl. Phys. IOSR-JAP 7 (2015) 52–55.

[30] E.G. Özdemir, E. Eser, Z. Merdan, Investigation of structural, half-metallic and elastic properties of a new full-Heusler compound–Ir2MnSi, Chinese J. Phys. 56 (4) (2018) 1551–1558.

[31] S. Krishnaveni, Electronic band structure analysis on newly proposed iridium based Heusler alloys in different exchange correlation potentials, J. Phys. Conf. Ser. 1172 (2019) 012041 (1).

[32] S. Krishnaveni, Halfmetallicity, mechanical and thermodynamic study on iridium based compounds by first principles calculations, Mater. Res. Express 6 (9) (2019) 096545.

[33] M. Gilleßen, R. Dronskowski, Maßgeschneidertes Und Analytik-ersatz: Über Die Quantenchemischen Untersuchungen Einiger Ternärer Intermetallischer Verbindungen (No. RWTH-CONV-113777), 2010. Fachgruppe Chemie.

[34] M. El Amine Monir, H. Ullah, H. Baltach, Y. Mouchaal, Half-metallic ferromagnetism in novel Rh_2-based full-Heusler alloys Rh_2FeZ (Z = Ga and in), J. Superconduct. Novel Magnetism 31 (2018) 2233–2239, https://doi.org/10.1007/s10948-017-4499-1.

[35] V.D. Buchelnikov, V.V. Sokolovskiy, O.N. Miroshkina, M.A. Zagrebin, J. Nokelainen, A. Pulkkinen, et al., Correlation effects on ground-state properties of ternary Heusler alloys: first-principles study, Phys. Rev. B 99 (1) (2019) 014426.

[36] J.P. Perdew, K. Burke, M. Ernzerhof, Generalized gradient approximation made simple, Phys. Rev. Lett. 77 (1997) 1396.

[37] S. Kirklin, J.E. Saal, B. Meredig, A. Thompson, J.W. Doak, M. Aykol, S. Rühl, C. Wolverton, The Open Quantum Materials Database (OQMD): assessing the accuracy of DFT formation energies", NPJ Comput. Mater. 1 (2015) 15010, https://doi.org/10.1038/npjcompumats.
[38] https://www.quantum-espresso.org/. Accessed 20 June 2019.
[39] P. Giannozzi, S. Baroni, N. Bonini, M. Calandra, R. Car, C. Cavazzoni, D. Ceresoli, G.L. Chiarotti, M. Cococcioni, I. Dabo, A. Dal Corso, S. de Gironcoli, S. Fabris, G. Fratesi, R. Gebauer, U. Gerstmann, C. Gougoussis, A. Kokalj, M. Lazzeri, L. Martin-Samos, N. Marzari, F. Mauri, R. Mazzarello, S. Paolini, A. Pasquarello, L. Paulatto, C. Sbraccia, S. Scandolo, G. Sclauzero, A.P. Seitsonen, A. Smogunov, P. Umari, R.M. Wentzcovitch, QUANTUM ESPRESSO: a modular and open-source software project for quantum simulations of materials, J. Condens. Mater. Phys. 21 (2009) 395502.
[40] H.J. Monkhorst, J.D. Pack, Special points for Brillouin-zone integrations, Phys. Rev. B 13 (1976) 5188.
[41] W. Voigt, Lehrbuch Der Kristallphysik, Taubner, Leipzig, 1928.
[42] A. Reuss, Z. Angew, Calculation of the flow limits of mixed crystals on the basis of the plasticity of monocrystals, Math. Mech. 9 (1929) 49.
[43] R. Hill, The elastic behaviour of a crystalline aggregate, Proc., Phys. Soc. Lond. A 65 (1952) 349.
[44] S. Baroni, S. De Gironcoli, A. Dal Corso, P. Giannozzi, Phonons and related crystal properties from density-functional perturbation theory, Rev. Mod. Phys. 73 (2001) 515.
[45] X. Gonze, C. Lee, Dynamical matrices, born effective charges, dielectric permittivity tensors, and interatomic force constants from density-functional perturbation theory, Phys. Rev. B 55 (1997) 10355.
[46] E.I. Isaev, QHA Project, 2013. Accessed May 25, http://qe-forge.org/qha.
[47] E. Şaşıoğlu, I. Galanakis, C. Friedrich, S. Blügel, Ab initio calculation of the effective on-site Coulomb interaction parameters for half-metallic magnets, Phys. Rev. B 88 (13) (2013) 13440.
[48] V. Stevanović, S. Lany, X. Zhang, A. Zunger, Correcting density functional theory for accurate predictions of compound enthalpies of formation: fitted elemental-phase reference energies, Phys. Rev. B 85 (11) (2012) 115104.
[49] M. Gillessen, Uber Die Quanten Chemischen Untersuch Ungeneiniger Ternarer Intermetallischer Verbindungen, PhD thesis, Oktober, Aachen, 2009.
[50] N. Arikan, H.Y. Ocak, G.D. Yıldız, Y.G. Yıldız, R. Ünal, Investigation of the mechanical, electronic and phonon properties of X_2ScAl (X = Ir, Os, and Pt) heusler compounds, J. Korean Phys. Soc. 76 (2020) 916–922.
[51] A. Birsan, V. Kuncser, First principle investigations of the structural, electronic and magnetic properties of predicted new zirconium based full-Heusler compounds, Zr_2MnZ (Z= Al, Ga and In), J. Magn. Magn. Mater. 406 (2016) 282–288.
[52] A.O. Oliynyk, E. Antono, T.D. Sparks, L. Ghadbeigi, M.W. Gaultois, B. Meredig, A. Mar, High-throughput machine-learning-driven synthesis of full-Heusler compounds, Chem. Mater. 28 (20) (2016) 7324–7331.
[53] S. Al, N. Arikan, A. İyigör, Investigations of structural, elastic, electronic and thermodynamic properties of X2TiAl Alloys: a computational study, Z. Naturforsch. B 73 (2018) 859–867.
[54] N. Arikan, O. Ornek, Z. Charifi, H. Baaziz, S. Ugur, G. Ugur, A first-principle study of Os-based compounds: electronic structure and vibrational properties, J. Phys. Chem. Solids 96-97 (2016) 121–127.
[55] M. Born, On the Stability of Crystal Lattices, I, Cambridge University Press, 1940, p. 160.
[56] R. Gaillac, P. Pullumbi, F. Coudert, ELATE: an open-source online application for analysis and visualization of elastic tensors, J. Phys. Condens. Matter 28 (2016) 275201.
[57] M. De Jong, W. Chen, T. Angsten, A. Jain, R. Notestine, A. Gamst, et al., Charting the complete elastic properties of inorganic crystalline compounds, Sci. Data 2 (1) (2015) 1–13.
[58] R.M. Hornreich, M. Kugler, S. Shtrikman, C. Sommers, Phonon band gaps, J. Phys. I France 7 (1997) 509.